Peptide and Protein Dynamics and Low-Temperature/DNP Magic Angle Spinning NMR

Peptide and Protein Dynamics and Low-Temperature/DNP Magic Angle Spinning NMR

Qing Zhe Ni[1], Evgeny Markhasin[1], Thach V. Can[1], Björn Corzilius[1,3], Kong Ooi Tan[1], Alexander B. Barnes[1,4], Eugenio Daviso[1,2,5], Yongchao Su[1,6], Judith Herzfeld[2], and Robert G. Griffin[1]*

[1] Department of Chemistry and Francis Bitter Magnet Laboratory, Massachusetts Institute of Technology, 77 Massachusetts Avenue, Cambridge, Massachusetts 02139, United States [2] Department of Chemistry, Brandeis University, Waltham, Massachusetts 02454, United States.

ABSTRACT: In DNP MAS NMR experiments at ~80-110 K, the structurally important $-^{13}CH_3$ and $-^{15}NH_3^+$ signals in MAS spectra of biological samples disappear due to the interference of the molecular motions with the ^1H decoupling. Here we investigate the effect of these dynamic processes on the NMR lineshapes and signal intensities in several typical systems: (1) microcrystalline APG, (2) membrane protein bR, (3) amyloid fibrils PI3-SH3, (4) monomeric alanine–CD_3 and (5) the protonated and deuterated dipeptide N-Ac-VL over 78-300 K. In APG, the 3-site hopping of the Ala-C_β peak disappears completely at 112 K, concomitant with the attenuation of CP signals from other ^{13}C's and ^{15}N's. Similarly, the ^{15}N signal from Ala-NH_3^+ disappears ~173 K, concurrent with the attenuation in CP experiments of other ^{15}N's as well as ^{13}C's. In bR and PI3-SH3, the methyl groups are attenuated at ~95 K while all other ^{13}C's remain unaffected. However, both systems exhibit substantial losses of intensity at ~243 K. Finally, with spectra of Ala and N-Ac-VL we show that it is possible to extract site specific dynamic data from the temperature dependence of the intensity losses. Furthermore, ^2H labeling can assist with recovering the spectral intensity. Thus, our study provides insight into the dynamic behavior of biological systems over a wide range of temperatures, and serves as a guide to optimizing the sensitivity and resolution of structural data in low temperature DNP MAS NMR spectra.

Introduction

Magic angle spinning (MAS) NMR spectroscopy is now established as a versatile and essential tool in structural biology.[1-9] In particular, advances in sample preparation, methodology,[10-19] and labeling strategies have dramatically improved the resolution of MAS spectra, thus making possible structural studies of large biomolecules not accessible with other techniques.[20-24] Nevertheless, the primary limiting factor of MAS NMR is its inherently low sensitivity. An approach to circumvent this limitation is operation at cryogenic temperatures, since the Boltzmann population scales as 1/T.[25-26] An even greater gain in sensitivity can be achieved by integrating dynamic nuclear polarization (DNP) into the MAS NMR experiments, where orders of magnitude enhancements of NMR signal intensities have been reported for peptide and protein samples.[27-30] This permits experiments that are otherwise difficult or impossible to perform.[31-35]

To take advantage of this increased sensitivity, DNP/NMR experiments at 80-120 K are becoming widely accessible and heavily utilized. However, to date, the tremendous sensitivity gain overshadows the effects of molecular motions present in the ambient and low temperature spectra. For example, in many cases, side chain and backbone resonances of structural importance are absent for reasons that are glibly referred to as "dynamics" but are not clearly delineated or understood. Early ^2H NMR studies on model compounds revealed threefold hopping (at 10^3-10^6 s^{-1}) by $-CD_3$ and $-ND_3^+$ groups at 130-200 K and 200–310 K temperatures, respectively[36-39] and there have been a few investigations of these threefold processes and twofold flips of aromatic rings in peptides and proteins at low temperatures.[40-47] However, to the best of our knowledge, none of them provide a detailed description of the effects of these processes on the accompanying loss in signal intensity in MAS spectra, especially in the 80-120 K regime. Furthermore, recent ob-

servation of heteronuclear polarization transfer under DNP has been attributed to methyl dynamics in proteins [48]. Thus, the purpose of the experiments reported here is to provide an overview of the global and site-specific spectral intensity losses as a function of temperature. Thus, we combine data from ^{1}H-$^{13}C/^{15}N$ cross polarization (CP), ^{13}C Bloch decay MAS experiments recorded from a series of temperature-dependent MAS NMR spectra on five systems including: (1) the microcrystalline tripeptide alanyl-prolyl-glycine (APG), (2) the membrane protein bacteriorhodopsin (bR), (3) amyloid fibrils of phosphatydinal-inositol-3-kinase SH3 domain (PI3-SH3), (4) monomeric $–CH_3$ and $-CD_3$ alanine and (5) the protonated and deuterated dipeptide N-acetyl-valyl-leucine (N-Ac-VL) over the temperature range 78-300 K.

In APG we find that the motion of the $-NH_3^+$ and $-CH_3$ interferes with ^{1}H decoupling and also compromises CP efficiencies, leading to specific and complete attenuation of spectral lines from these two groups at ~173 K and ~112 K, respectively. In addition, these intensity losses propagate throughout the sample, causing a global loss of spectral intensity. At temperatures around 80 K, the interfering motions approach the rigid lattice limit and the signal intensity fully recovers. In this regime, the gain in signal intensity is purely due to the Boltzmann factor.

Two classes of larger protein systems commonly studied at low temperature and with DNP include membrane and amyloid proteins.[49-52] Examples of these systems include bR in its native purple membrane and PI3-SH3. In both of these cases, the signal minimum due to the dynamics of $–CH_3$ groups occurs at a lower temperature (95 K) and appears to be localized as opposed to the case of APG. In addition, other spectral regions such as the carbonyl and aromatic resonances are not affected and exhibit improved signals. Finally, we show that intensity losses due to dynamic process can be partially and in some cases completely recovered by the introduction of ^{2}H labeling. In particular, the introduction of $–CD_3$ groups in Ala, N-Ac-VL and the use of perdeuterated bR permit observation of these groups in cases where spectral lines from the $–CH_3$ moiety are completely absent.

EXPERIMENTAL

Sample Preparation

Both uniformly $^{13}C,^{15}N$-labeled and ^{15}N-labeled APG samples were diluted to 10% with the corresponding natural abundance APG to suppress any intermolecular couplings. This was accomplished by dissolving the mixture of labeled APG/ natural abundance APG in a minimal amount of water (~ 45 mg/ml) followed by slow crystallization in a desiccator, and crystals forming in about a week. 40 mg of each APG samples was packed into a 4 mm Revolution NMR zirconia rotor.

Bacteriorhodopsin (bR), in its native purple membrane, was purified from *Halobacterium salinarum* grown in uniformly $^{13}C,^{15}N$-labeled peptone medium[53]. Peptone was obtained from the anaerobic acid hydrolysis of *Methylophilus methylotrophus* cells grown on ^{13}C-labeled methanol and ^{15}N-labeled ammonium sulfate.[54] The purple membranes were isolated using the method of Oesterhelt and Stoechenius[55]. The sample was washed 3 times with 300 mM guanidine hydrochloride at pH 10.0. The sample was pelleted after every wash by centrifugation for 2 hours at ~43,000 g. The washed pellet was mixed with 5mM AMUPol[56] or 15mM TOTAPOL[57] in "DNP juice" consisting of d_8-glycerol/D_2O/H_2O (60/30/10 volume ratio) and centrifuged once more.

The phosphatidyl-inositol-3-kinase SH3 domain PI3-SH3 fibril sample was uniformly $^{13}C,^{15}N$-labeled at the F, V, Y and L residues. The fibrils were grown from a solution of monomeric protein by incubation at pH 2.0 and 25°C for 14 days.[58] "DNP juice" was adjusted to pH 2.0 and supplemented with 15 mM TOTAPOL was added to the gel-like fibrils for cryoprotection and DNP experiments. Both bR and PI3-SH3 samples were packed into a 4 mm sapphire rotor for DNP/NMR experiments.

[U-$^{13}C,^{15}N$] and [-CD_3-U-$^{13}C,^{15}N$] alanine were purchased from Cambridge Isotope Laboratories (CIL) and dissolved in water then crystallized in a desiccator. [U-$^{13}C,^{15}N$] *N*-acetyl-L-Val-L-Leu (N-Ac-VL) and [1,2-^{13}C] acetic anhydride were purchased from CIL. N-Ac-VL was synthesized by New England Peptide (Gardner, MA), using

standard solid-phase methods and purified by HPLC. N-Ac-VL was crystallized from a 1:1 (v/v) H_2O:acetone solution.

NMR spectroscopy

MAS spectra were recorded using a custom-designed triple resonance (^1H, ^{13}C, ^{15}N) cryogenic MAS probe equipped with a sample exchange system[59] on home-built NMR spectrometer operating at 380 MHz ^1H frequency (courtesy of Dr. D. J. Ruben). Two types of 1D NMR experiments were conducted for APG: ^1H-^{13}C/^{15}N cross polarization (CP) and ^{13}C Bloch decay. For CP experiments, a spin-lock field of 50 kHz was employed on the proton channel. Experimental parameters including: recycle delay, CP Hartmann Hahn matching conditions, CP duration and TPPM decoupling have all been optimized for all temperature dependent experiments. ^1H TPPM decoupling fields $\omega_{1H}/2\pi$ = 83 kHz or 100 kHz and $\omega_r/2\pi$ = 4.83 kHz were used unless stated otherwise.

Liquid nitrogen boil-off gas was used for both the bearing and drive gas streams, and the spinning frequency was controlled by a Bruker MAS controller[59]. Both bearing and drive streams were cooled using a custom-designed heat exchanger, and the temperature was subsequently controlled using heating elements inside vacuum jacketed transfer lines with two PID controllers (Lakeshore, Westerville, OH). The sample temperature was monitored using a fiber optic temperature sensor (Neoptix, Quebec, Canada) that extends to the inside of the MAS stator. The fiber optic thermometers were calibrated by immersion in liquid nitrogen at 77 K. Note, during MAS experiments, we have consistently recorded temperatures in the range 72 K-77 K presumably due to Joule-Thompson cooling on the expansion of the N_2 gas from the jets of drive cup and bearings of the stator.

DNP experiments

In order to investigate methyl group dynamics at DNP temperatures, ^1H, ^{13}C, ^{15}N CP and homonuclear experiments were performed using a home-built DNP gyrotron instrument operating at 250 GHz / 380 MHz with ~14 W of microwave power.[60-61] Enhancement factors (ε) were calculated by comparing the signals obtained with and without μw irradiation.

Simulations

The simulations of the Ala–CH_3 group dynamics in APG (**Figure 7)** were performed using GAMMA[62] with 100 powder orientations chosen using ZCW scheme.[63] Details of the parameters used can be found in SI. In order to simulate the three-site hopping mechanism, the simulations were carried out in a composite Liouvillian space that facilitates mutual-exchange mechanism. The dimensions of the exchange matrices for the four-spin CH_3 and CD_3 spin systems are 256 x 256 and 2916 x 2916 respectively. The amount of time required to simulate the FID of one crystallite orientation using one CPU core is ~1 minute and ~1.5 days for CH_3 and CD_3 respectively. All simulations took ~2 weeks to compute using ETH Brutus cluster with 384 CPU cores. The parameters chosen for the simulations are $\omega_r/2\pi$=4.651 kHz, TPPM decoupling $\omega_{1H}/2\pi$= 83 kHz with 6.9 μs pulses and phases ±15 degree. The size of the quadrupole coupling used for ^2H nuclei is 167 kHz.

RESULTS

The 1D ^{13}C spectra in **Figure 1** illustrate the spectral resolution of two microcrystalline APG samples with differing isotopic labeling schemes at 80 K. In both cases, the spectra exhibit resolution comparable to that obtained at room temperature. Specifically, **Figure 1a** shows a ^{13}C CP MAS NMR spectrum of [U-^{12}C,^{15}N]-APG and in the absence of ^{13}C-^{13}C *J*-couplings, the linewidth of the Gly-C_o is as narrow as 27 Hz (0.28 ppm). In comparison, the linewidths in the spectrum of [U-^{13}C,^{15}N]-APG (**Figure 1b**) increase by a factor of two or more primarily due to one bond *J*-couplings and higher order cross terms that arises from the denser ^{13}C network. Nevertheless, resolved *J*-splittings (~50 Hz) can still be distinguished in two out of three carbonyls, each of which has only one *J*-coupled neighboring ^{13}C. On the other hand, each ^{13}C in the aliphatic region is *J*-coupled to multiple neighbors, which obscures the splitting. The aliphatic carbons also have stronger CH dipolar coupling than that of

carbonyl carbons, and would require stronger decoupling and higher spinning frequencies to be averaged out effctively. The data confirm that the optimal resolution in MAS spectra can be obtained with sparsely labeled ^{13}C samples.[64] In addition, they demonstrate that high resolution in well-ordered materials can be obtained at cryogenic temperatures (~ 80 K).

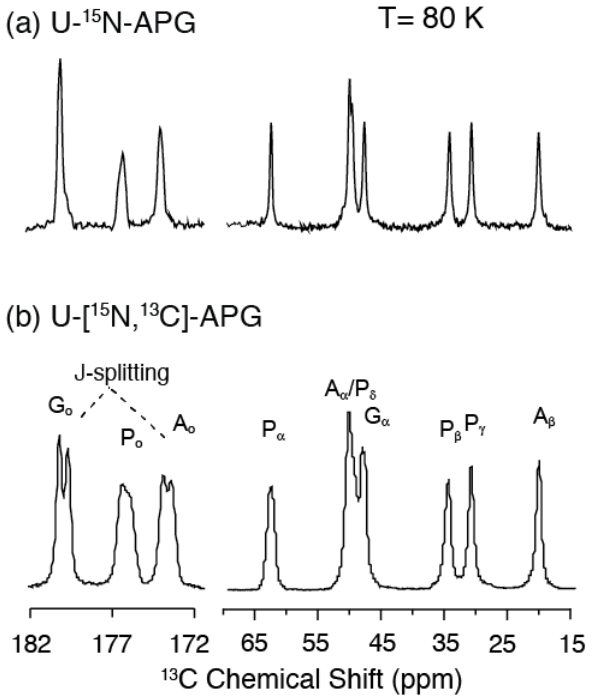

Figure 1. ^{13}C CP-MAS spectrum of [U-^{15}N] APG (a) and [U-^{13}C,^{15}N] APG (b) at 80 K. Both samples were diluted to 10% in unlabeled APG to minimize the intermolecular couplings. The linewidth of the Gly-C_o is 27 Hz (0.28 ppm). In (b) the linewidth is broadened by ^{13}C-^{13}C *J*-coupling evident in the doublet splitting in the carbonyl region with the Gly-C_o and Ala-C_o showing one bond C_α-C_o *J*-couplings of ~50 Hz. The fact that these resonances are not resolved in the aliphatic region is likely due to the presence of multiple *J*-couplings.

Figure 2 illustrates the temperature dependence of the ^1H-^{13}C/^{15}N CP-MAS spectra acquired in the range from 73 K to 295 K, where we observe several interesting spectral changes. First, in the transition between regions I and II at 225 K, there is a doubling in all of the side chain signals that is especially obvious on the Ala-C_β line ($\delta \approx 18$ ppm at 295 K), as well as Pro-C_β and Pro-C_γ (30 ppm and 35 ppm at 295 K, respectively). A recent calorimetric study of APG crystals revealed that the spectral changes at 225 K, although in the vicinity of the famous protein glass transition,[65] are likely the result of a polymorphic phase transition[66]. Similar spectral changes at ~200 K were observed for the peptide N-*f*-MLF-OH.[32] Second, in region III, the intensity of Ala-C_β exhibits a local minimum that coincides with the disappearance of the ^{15}N signal from the -NH_3^+ group at ~173 K. Third, at lower temperatures, in region IV between 148 K and 96 K, a more significant loss of Ala-$^{13}C_\beta$ signal intensity occurs. The intensity decreases dramatically and the Ala-$^{13}C_\beta$ line disappears into the baseline at ~112 K, and there is a concurrent loss of spectral intensity in the ^{15}N spectra at this temperature. We attribute the two signal minima in regions III and IV at ~173 K and ~112 K to the threefold hopping rates of the -NH_3^+ and -CH_3 groups, respectively, matching the ^1H decoupling frequency. Finally, at lower temperatures the hopping rate enters the slow exchange limit and the –CH_3 and –NH_3^+ lines reappear, narrow and the intensity recovers fully at 73 K.

The temperature dependence of the signal intensity is a product of the Boltzmann factor, which has a T^{-1} dependence, and the intensity loss due to molecular motions, which varies with temperature. In order to isolate the effect of molecular dynamics, the contribution from the Boltzmann factor is removed by multiplying the integrated signal intensity by the corresponding temperature. **Figure 3a** shows the normalized signal intensity of Ala-C_β (-CH_3 group) with (red solid circles) and without (blue open circles) the correction for the Boltzmann factor. To correct for the Boltzmann factor, the normalized intensity was calculated as $(I \cdot T)/(I_0 \cdot T_0)$ where I_0 is the intensity at the highest temperature T_0, where experiments were performed and I is the intensity at temperature T. To facilitate data presentation, without the correction for the Boltzmann factor, the normalized intensity was calculated differently as (I / I_0) to where I_0 the intensity at lowest temperature at which we perform experiments. Note that the integrated signal intensities were adjusted when necessary by their relative ^1H or ^{13}C T_1's measured at each temperature and incorporated into the intensity calculations. T_{1H} and T_{13C} values are plotted as a function of temperature in **Figure S1** in the supporting information. The minima at ~112 K and ~173 K in **Figure 3**

are visible even without this correction and are greatly amplified with the correction. Below 90 K and above 225 K, the adjusted signals in red

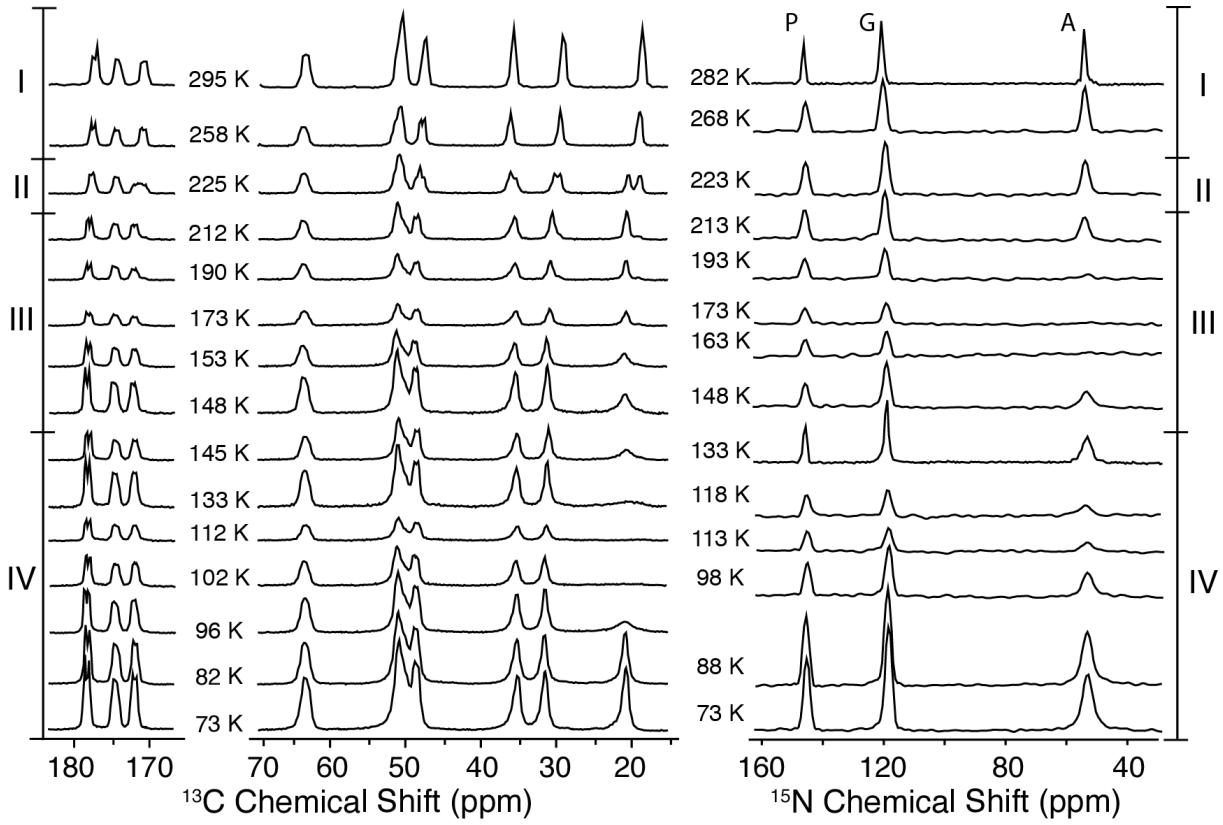

Figure 2. Temperature-dependent ^{1}H-^{13}C CP (left column) and ^{1}H-^{15}N CP (right column) spectra of [U-^{13}C,^{15}N] APG. Several important spectral changes are observed. In region (III), between 213 K and 148 K, the intensity of the Ala-NH_3^+ peak is buried under the noise level at ~ 173 K, which couples with the partial attenuation of the ^{13}C spectrum. Region (IV), below 148 K, exhibits the disappearance of the Ala-CH_3 signal at ~113 K, coincident with the signal dip in the ^{15}N spectrum. The spectral changes are further analyzed in **Figure 3**. The spectra were acquired with $\omega_r/2\pi$ = 4.83 kHz, $\omega_{1H}/2\pi$ = 83 kHz for TPPM decoupling.

are essentially the same, indicating that the signal intensities are unaffected by the effect of molecular dynamics in these regions. In particular, the signal intensity in these regions follows closely the T^{-1} dependence, resulting in a factor of 4 times higher intensity at 73 K compared to 295 K. **Figure 3b** illustrates that other sites such as Pro-C_α, and Gly-C_o also exhibit two signal minima in ^{1}H-^{13}C CP experiments and the entire spectrum is uniformly attenuated at 112 K and 173 K. **Figure 3c** presents the data from the single-pulse ^{13}C Bloch decay signals detected with ^{1}H decoupling that show a minimum at 112 K, and a set of ^{13}C Bloch decay spectra is included in **Figure S2**. Furthermore, at this temperature the Ala-CH_3 is also completely attenuated **(Figure 3a)**, whereas other sites are nearly unaffected. In combination, the data in **Figure 3b** and **3c** suggest that the signal minimum at ~112 K is associated with the threefold hopping rate of the Ala–CH_3, which approximates to the Rabi frequency of the ^{1}H RF fields during decoupling and/or CP. The minimum at ~173 K is attributed to the hopping of the Ala-NH_3^+ which manifests itself in the disappearance of its ^{1}H-^{15}N CP signal as shown in **Figure 3d**. In comparison to the ^{1}H-^{13}C CP data (**Figure 3b**), the ^{1}H-^{15}N CP data also exhibit two minima but in reverse intensity order: nearly uniform signal attenuation at ~112 K and complete signal attenuation of Ala-NH_3^+ at ~173 K.

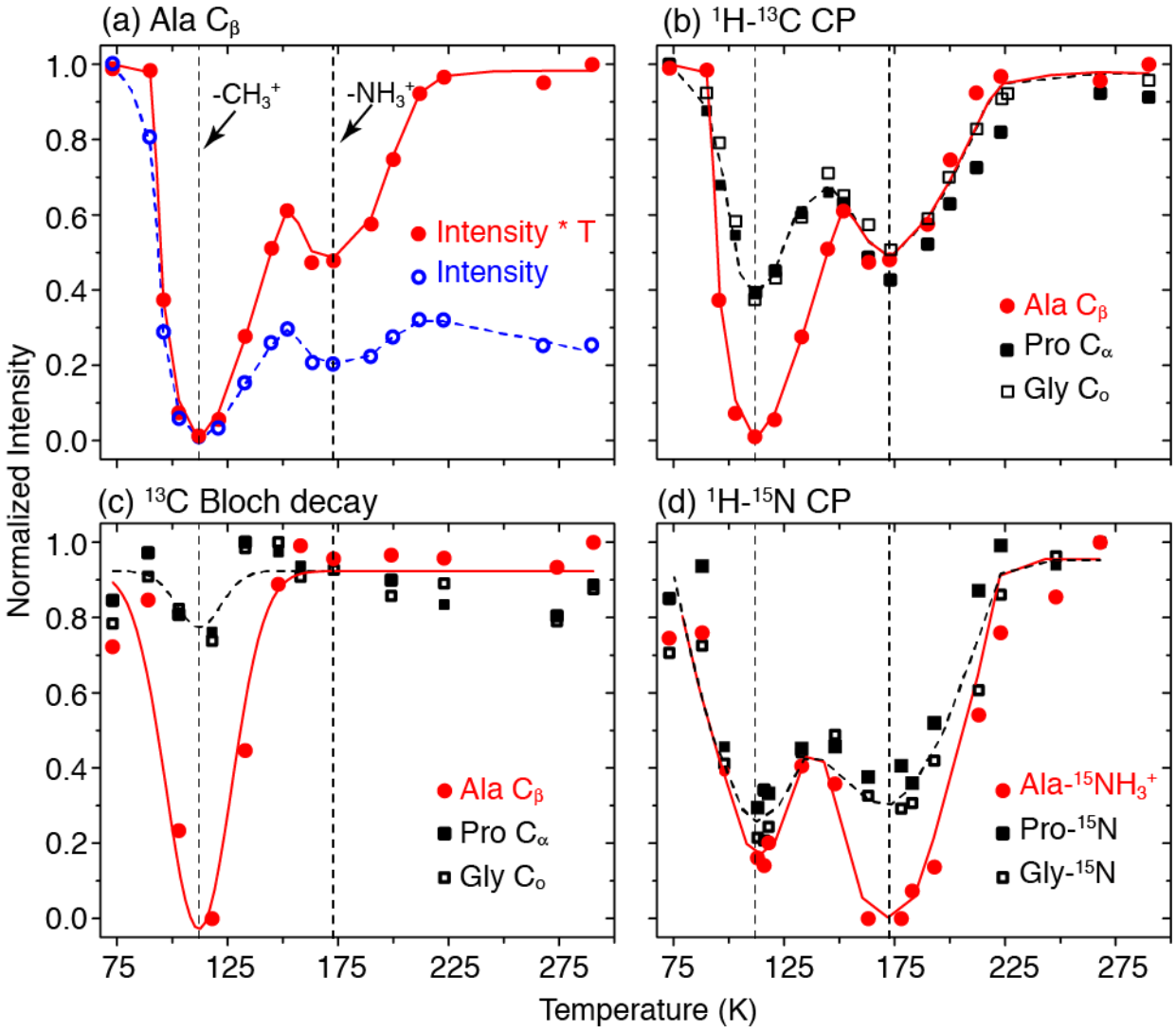

Figure 3. Temperature dependence of the integrated peak intensities of [U-^{13}C,^{15}N]-APG. The vertical dashed lines indicate the minima in the signal intensities at ~112 K and ~173 K due to the hopping of -CH_3 and -NH_3^+, respectively. (a) Ala-C_β from ^{1}H -^{13}C CP with (red solid circles) and without (blue open circles) Boltzmann correction at each temperature. (b) Adjusted spectrum intensities of several peaks of APG plotted as a function of temperature from ^{1}H -^{13}C CP. Again, notice the two minima, ~112 K where the Ala-C_β peak broadens beyond detection, and ~173 K. (c) ^{13}C Bloch decay experiments show the first minimum, indicating interference between methyl hopping and ^{1}H decoupling. (d) Spectral intensities of ^{1}H -^{15}N CP alanine NH_3^+as a function of temperature. The second minimum in (b) is due to the hopping of Ala-NH_3^+ group.

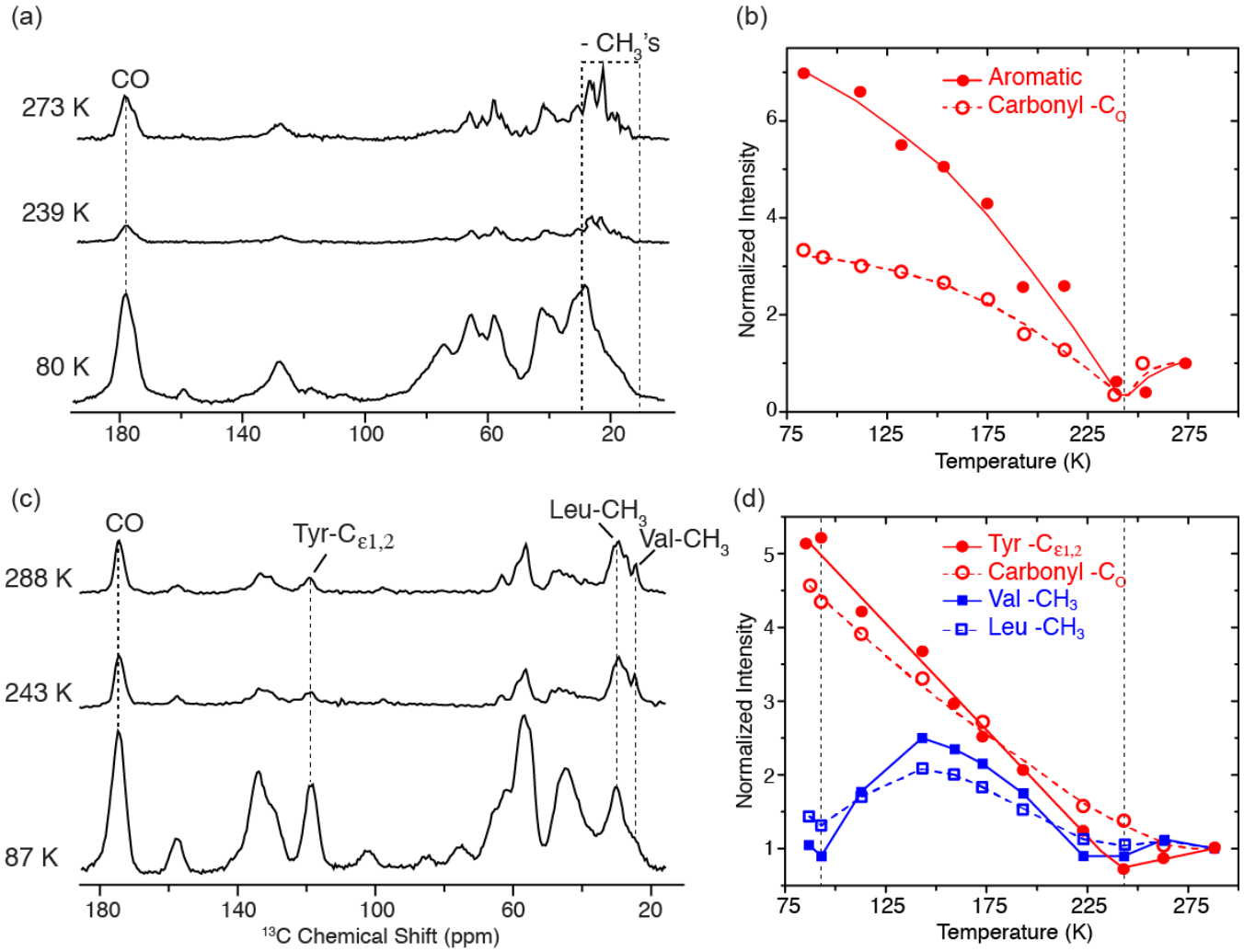

Figure 4. Temperature-dependent ^{1}H-^{13}C CP spectra of (a) [U-^{13}C,^{15}N] bacteriorhodopsin and (c) [^{13}C,^{15}N-FVYL]-PI3-SH3 amyloid fibrils without Boltzmann correction. In (b) and (d) we show plots of normalized intensities for carbonyl, aromatic and aliphatic regions in bR and PI3-SH3 fibrils as a function of temperature. Both carbonyl and aromatic experience a minimum in intensity around 243 K followed by a steady increase as the temperature is decreased for both systems. The intensity of –CH_3's in the valines and leucines in PI3-SH3 also reveals a minimum at ~243 K, followed by a second minimum at ~95 K, where the intensity losses are again due to –CH_3 hopping interfering with ^{1}H decoupling and spin-lock fields. Both samples were cryoprotected in d_8-glycerol/D_2O/H_2O (60/30/10 volume ratio). Full sets of spectra at different temperatures are provided in **Figure S3** and **S4**. The spectra were acquired with $\omega_r/2\pi$ = 4.83 kHz for bR and 7 kHz for PI3-SH3. In both cases, $\omega_{1H}/2\pi$ = 83 kHz for TPPM decoupling.

Motivated by the dramatic changes in signal intensities in the APG spectra, we extended our studies to the membrane protein bR, and to amyloid fibrils formed by PI3-SH3, to determine if a similar behavior is observed in these systems. **Figure 4a** illustrates that attenuation of methyl ^{13}C resonances occurs in [U-^{13}C,^{15}N]-bR. However, because of spectral overlap in this 248 amino acid, uniformly ^{13}C/^{15}N labeled protein, the extraction of accurate intensity data for these resonances is imprecise. Multidimensional experiments at higher fields are required to obtain better resolution. In contrast, the spectra in **Figure 4c** of [^{13}C,^{15}N-FVYL]-PI3-SH3 are greatly simplified, which permits the extraction of the intensity of different functional groups, especially the Val-CH_3 and Leu-CH_3. In general, the spectra show that the overall intensity of carbonyl and aromatic ^{13}C's in both samples increases as temperature decreases except around 243 K (**Figure 4b** and **4d**). In addition, the methyl groups exhibit another minimum at ~95 K in the case of

[^{13}C,^{15}N-FVYL]-PI3-SH3, but the intensities of the two –CH_3 containing residues are partially recovered at 87 K and are expected to fully recover at lower temperatures. Incorporation of DNP into the experiments in this temperature regime will, in addition to the Boltzmann factor, boost the sensitivity. In **Figure S5,** we show 1D ^{1}H-^{13}C CP spectra of [^{13}C,^{15}N-FVYL]-PI3-SH3 obtained with a signal enhancement of 35. A 2D RFDR spectrum of [^{13}C,^{15}N-FVYL]-PI3-SH3 fibril with τ_{mix}=1.6 ms was acquired in approximately 4 hours. Without DNP, the same spectrum would require one month to achieve the same S/N.

In **Figure 4b** and **4d**, the intensities are normalized to those obtained at 275 K for bR and 283 K for PI3-SH3. We note that the normalized intensities of the aromatic ^{13}C's at ~ 80-90 K can be larger than the contribution from the Boltzmann factor. This is due to the fact that at 300 K there is already a significant loss in signal intensity in aromatic ring spectra due to the twofold ring flips,[67-70] which affects the polarization transfer during CP and interferes with decoupling. This phenomenon was observed in N-*f*-MLF-OH where the δ, δ' and ε, ε' signals from the Phe ring are absent in the 300 K 1D spectra. They start to reappear at 250K-225K and are fully developed at lower temperatures.[32] In addition, in ZF-TEDOR spectra of PI3-SH3, the aromatic region is essentially empty at 300 K but is intense and well resolved at 90 K.[71] Thus, the broad signal minimum around 243 K probably extends to the higher temperatures, ~ 280 K. Note also that protein samples used for DNP are cryoprotected by the glass-forming mixture of glycerol/water (60/40 volume ratio), as it is the case for the bR and PI3-SH3 samples used in our study. Therefore, the signal minimum at 243 K coincides with the freezing of the glycerol/water mixture and a slowing of the twofold flips of the 24 aromatic rings in bR. We also note that this temperature is close to that of the protein glass transition, although it is generally centered at the somewhat lower temperature (~200 K).

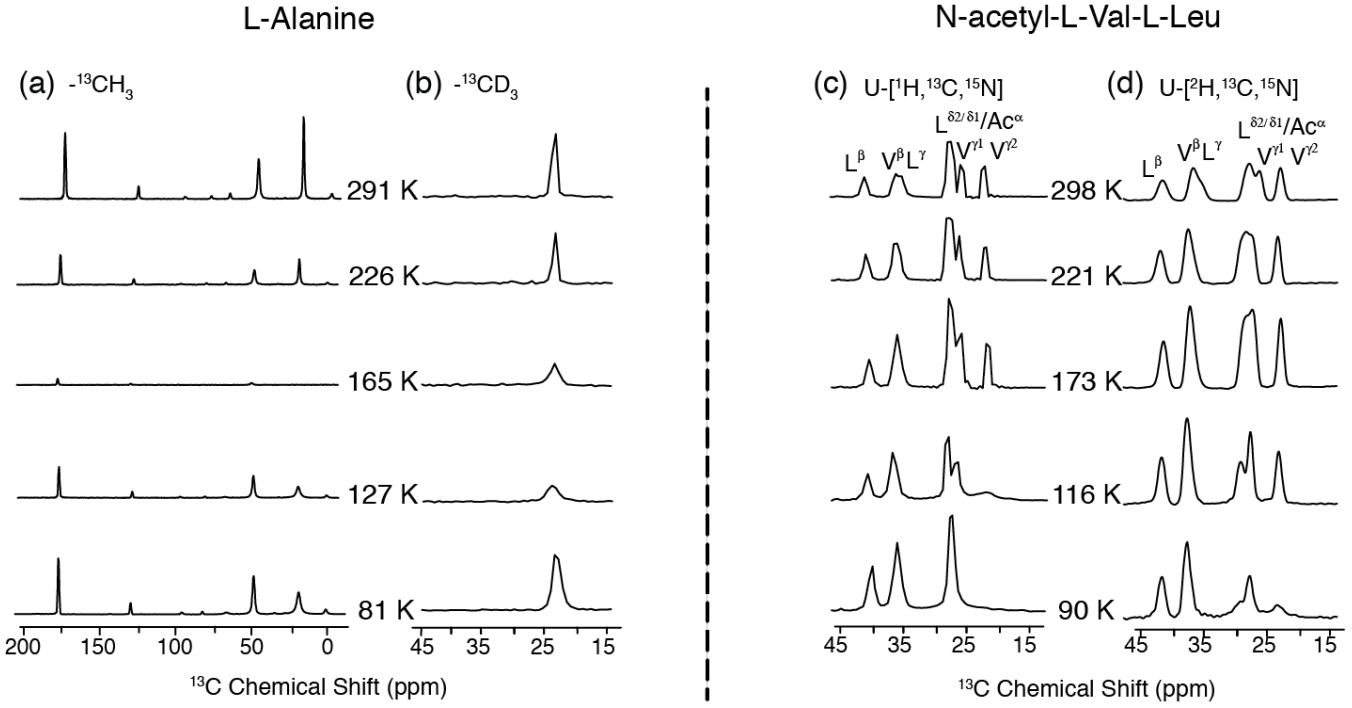

Figure 5. Temperature dependent ^{13}C MAS spectra of (a) [U-^{13}C,^{15}N]-Ala with a $^{13}CH_3$; (b)Ala-$^{13}CD_3$; (c) [U-^{1}H,^{13}C,^{15}N] N-acetyl-L-Val-L-Leu (d) [U-^{2}H,^{13}C,^{15}N] N-acetyl-L-Val-L-Leu. The spectra were acquired with $\omega_r/2\pi$ = 6.2 kHz, $\omega_{1H}/2\pi$ = 100 kHz for TPPM decoupling.

It would clearly be desirable to recover the signal loss due to the interference between molecular dynamics and decoupling, and accordingly, we have examined the possibility of labeling methyl groups as $-CD_3$'s.[36-37] The rationale behind this approach is that the 1st order ^2H quadrupole coupling is inhomogeneous, the 2nd order ^2H coupling is small at high fields, and ^2H-^2H dipole couplings, proportional to g_I^2, are a factor of 42 smaller than ^1H-^1H dipole couplings. Thus, MAS itself should average the ^2H-^2H and ^2H-^{13}C dipolar couplings and attenuate the intensity losses. **Figure 5** shows temperature-dependent spectra obtained from the monomeric amino acid alanine containing either a $-CH_3$ or $-CD_3$ group. As expected the ^{13}C MAS spectra obtained from Ala-$^{13}CH_3$ exhibit dramatic intensity losses around 165 K. Note that the intensity also decreases uniformly across the spectrum and both the C_α and C_o resonances are effectively suppressed as was the case in APG (**Figure 2**). However, with the $-^{13}CD_3$ present, the Ala methyl line is not suppressed at 165 K and the intensity recovers at 81 K. Nevertheless, there is still considerable intensity loss at 165 K, and, as discussed below, this is probably due to the $-CD_3$ methyl hopping rate ($\sim 10^4$-10^5 s^{-1}) being similar to magic angle spinning frequency. By interpolating the data from the Arrhenius plot reported by Beshah et al. for Ala–CD_3, we obtain hopping rates of 1.4 x 10^5 at 165 K and 1.6 x 10^3 at 127 K,[38] which confirms our hypothesis.

To explore the intensity losses in two other amino acids, namely Leu and Val, we recorded spectra of protonated and $-CD_3$ labeled N-Ac-VL. As shown in **Figure 5c**, the Val g_1 and g_2 lines in protonated N-Ac-VL exhibit significant intensity losses and are absent in the spectrum for T<116 K. Note also that the line from $V^{\gamma 2}$ disappears in the interval 116-173 K whereas the $V^{\gamma 1}$ line persists to ~116 K. This behavior is consistent with the fact that the threefold hopping rates, measured with ^2H spectra, for the two $-CH_3$ groups in Val differ by about an order of magnitude[38]. Specifically, in N-Ac-DL-Val they are 4.8 x 10^5 and 2.8 x 10^6 at 118 K, and therefore, the signal intensities of the methyl groups at 116 K (**Figure 5d**) are not severely attenuated and still detectable as the hopping rates are ~1-2 order of magnitude away from the interference regime ($\sim 10^4$-10^5 s^{-1}). In contrast, the Leu–CH_3 line does not lose intensity even at 90 K and it can potentially be used for distance measurements at low temperatures. In deuterated N-Ac-VL, both groups are present at 90 K but with reduced intensity.

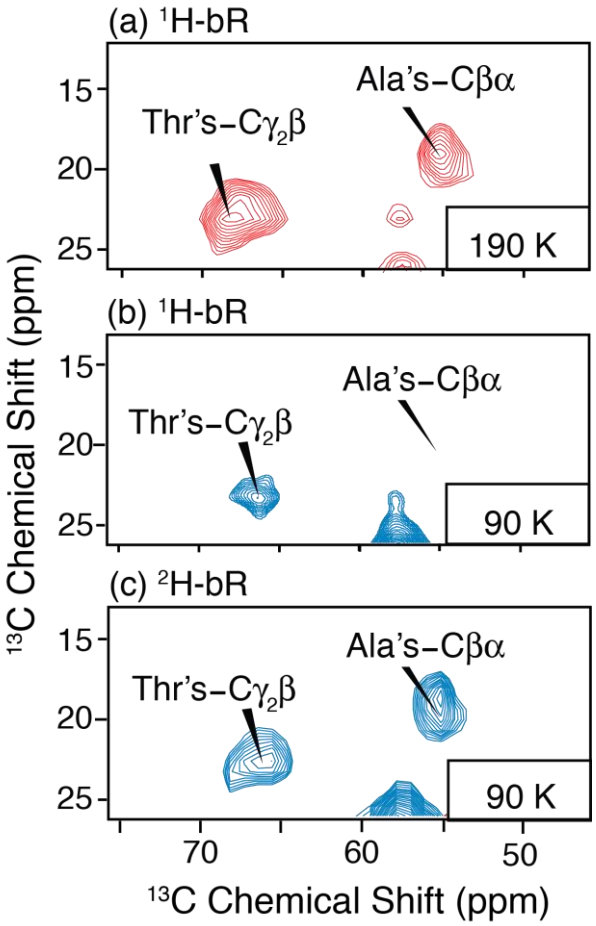

Figure 6. 2D DNP enhanced ^{13}C-^{13}C RFDR spectra of (A) U-^1H,^{13}C,^{15}N bR doped with 5 mM AMUPol at 190 K, (B) 92 K and (C) 2D RFDR of U-^2H, ^{13}C,^{15}N bR containing 15mM TOTAPOL at 92 K. (B) and (C) were acquired with DNP microwave irradiation. Enhancements of 75 and 71 were obtained, respectively. All spectra were acquired with 2ms mixing, 30 kHz ^{13}C pulses and 100 kHz ^1H decoupling and spinning frequency $\omega_r/2\pi$= 7 kHz at $\omega_{0H}/2\pi$= 380 MHz. Both experiments took 7 hours with 6 s recycle delay, 128 t_1 increments, and 32 scans per increment.

In DNP enhanced spectra of uniformly labeled bR, the intensity of methyl containing residues is also reduced. **Figure 6a** shows a 2D RFDR spectrum of ^1H uniformly labeled bR at 190 K with cross peaks corresponding to the 29 Ala and 18 Thr $-CH_3$'s in bR that are not re-

solved at 380 MHz. In contrast, at 90 K (**Figure 6b)** the Ala $C_{\beta\alpha}$ cross-peaks is no longer observed in the ^{1}H bR sample while it is detected in the ^{2}H uniformly labeled bR. Similarly, $Thr_{\gamma 2\beta}$ cross-peaks are partially attenuated in the ^{1}H spectrum compared to that at 190 K, but it is fully recovered in the spectrum of ^{2}H bR. This further verifies that an effective solution of methyl group attenuation could involve deuteration.

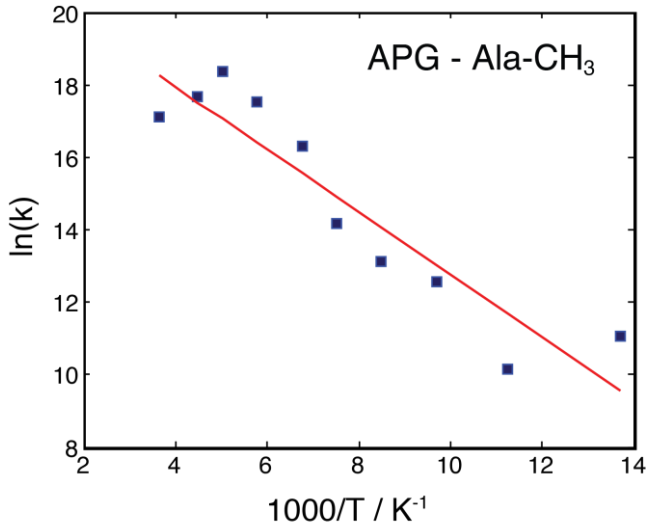

Figure 7. Arrhenius plot of three-site hopping rate of the Ala $–CH_3$ group in APG. The least-square fit (red line) yields an activation energy E_a of 7.2 ± 1 kJ/mol and pre-exponential constant A of ~ 2 x 10^9 s^{-1}.

Although the loss of signal intensity of the methyl groups at low temperature impedes many NMR experiments, including distance measurements, it encodes useful information the site-specific about the dynamics of group, for instance the activation energy, E_a. The activation energy contains rich details about the local chemical and structural environment, and they can be extracted by first comparing experimental data at different temperatures with numerical simulations. **Figure 7** shows the Arrhenius plot of the $–CH_3$ group hoping rates of alanine extracted from simulations of the signal intensities in APG measured by observing ^{13}C signals directly using a Bloch decay in the presence of ^{1}H decoupling. (data from **Figure 3c)**. The least-square fit yields an activation energy E_a of 7.2 ± 1 kJ/mol. This value is lower than the literature value of 20.0 kJ/mol[39] obtained for the monomeric amino acid alanine. The activation energy of the $–CH_3$ group in alanine is higher than that in the APG probably due to tighter crystal packing and thus more restricted rotation. Hence, the higher barrier for threefold hopping. However, this analysis is complicated by the fact that the methyl group is not strictly an isolated system, i.e. it is coupled to the nearby proton bath, especially the $–NH_3^+$ group via spin diffusion. A more detailed study of this effect on the activation energy can be performed by deuteration of the NH_3^+ group.

DISCUSSION

It is well known that the hopping rates of $-CH_3$ and $-NH_3^+$ groups can be measured precisely by analyzing the ^{2}H lineshape of the deuterated analogs of these groups.[36-39] Alternatively, Long *et al.* showed a strong correlation between the intensity of Bloch decay signals of ^{15}N and the hopping rate in $-NH_3^+$.[37] Using the same approach, we acquired ^{13}C Bloch decay signals (**Figure 3c**) and assigned the signal minimum at ~112 K to the interference between the methyl group hopping and the ^{1}H decoupling. Furthermore, the small signal attenuation (10%) of Pro-C_α and Gly-C_o from Bloch decay experiments (**Figure 3c**) cannot account for the large signal loss (60%) of the same resonances from CP experiments (**Figure 3b**), suggesting that the methyl group hopping also causes inefficient CP at this temperature. This suggests that the hopping rate of the methyl group in APG at ~112 K is ~10^4-10^5 s^{-1}, i.e. same order of magnitude as the MAS frequency and/or ^{1}H decoupling regime. The hopping rate can be extracted from the fitted Arrhenius plot (**Figure 7**) and we obtained a hopping rate of ~7 x 10^5 s^{-1}, thus confirming our hypothesis.

In practice, the decoupling field and the spin-locking field are very close in strength. Thus, it is expected that interferences between these Rabi fields and the 3-site hopping occur at the same temperature. Interference between the spin-locking field and the molecular dynamics is clearly the dominant mechanism responsible for the signal minimum at ~173 K in the ^{1}H-^{13}C CP data, (**Figure 3b**) which does not appear in the ^{13}C Bloch decay data (**Figure 3c**). At this matching condition, the spin-lock is inefficient for methyl ^{1}H's, causing a short ^{1}H $T_{1\rho}$. Furthermore,

due to rapid ^{1}H-^{1}H spin diffusion and the combination of intra- and inter-molecular contacts, the effect of a short $T_{1\rho}$ of the methyl ^{1}H's readily distributes itself throughout the molecule, resulting in a uniform signal loss at ~173 K in the ^{1}H-^{13}C CP data (**Figure 3b**). In contrast, the destructive interference effect on the decoupling appears to be more localized to the -CH_3 and -NH_3^+. This is apparent in the signal minimum at ~112 K in **Figure 3b** and **3c** as well as in the signal loss at ~173 K in the ^{1}H-^{15}N CP data, (**Figure 3d**) which is due to interference of -NH_3^+ hopping with both the decoupling and spin-lock fields.

The diffusive hopping of -CH_3 causes the first minimum at ~112 K, and the second at ~173 K is also caused by the similar phenomenon involving the -NH_3^+ group. The temperature or hopping rate at which the signal intensity is minimum is governed by both the E_a and the pre-exponential factor of the Arrhenius equation, *A*. However, if the values of *A* are comparable, then by comparing the previously published E_a values, one can predict the temperature range at which the intensity is minimum. The higher activation energy of the -NH_3^+ group is due to its ability to form hydrogen bonds.[37] For example, the E_a in Ala for -ND_3^+ is 40.5 kJ/mol,[37] whereas that for the -CD_3 group is 20.0 kJ/mol.[39] Long has shown the E_a of CD_3 and CH_3 groups are comparable. Similar to the case of -CH_3, Long *et al.* shows that the hopping rate of -NH_3^+ in Ala reaches 5 x 10^4 s^{-1} at 243 K, which is significantly higher than 173 K implied by our data, pointing to lower activation energy in APG, given that the values of *A* are comparable in both cases.

Our hypothesis on the correlation between molecular packing/ flexibility and the E_a is further supported by the data on larger systems including the membrane protein bR (**Figure 4a** and **4b**) and amyloid fibrils of PI3-SH3 (**Figure 4c** and **4d**). In contrast to the tripeptide APG, in bR and PI3-SH3 the hopping effect appears to be localized to the methyl groups. In [FVYL-^{13}C,^{15}N] PI3-SH3, a sample in which only methyl groups of Val and Leu are labeled, we are able to observe the minimum in the intensity of the –CH_3 groups at ~95 K, compared to ~112 K in APG, suggesting a lower E_a.

Our observations have a direct implication for the application of DNP to problems in structural biology. Carbonyl ^{13}C's, together with the aromatic side chains, are the least affected by the molecular dynamics and exhibit excellent sensitivity at low temperatures. This validates the approach using low temperature DNP to obtain long-range intermolecular distances involving aromatic side chains[71]. Similarly, methyl groups are of proven importance in measuring long-range contacts in proteins due to their position at the termini of many amino acid side chains. Interestingly, as demonstrated by the data here, one cannot use DNP experiments in the 80-120 K temperature range to measure distances associated with certain protonated (–CH_3) methyl groups. As hinted by the partial recovery of the methyl carbons at 87 K in **Figure 3 and 4,** the brute force solution to this problem is to perform experiments at even lower temperatures, which would then require cooling using liquid helium. A promising alternative approach is to fully or partially deuterate the methyl groups and it was demonstrated some time ago that full deuteration largely prevents the intensity losses observed here.[36] Thus, the benefit of this approach is two-fold. First, it circumvents the detrimental intensity losses while maintaining sufficient CP from adjacent protons. Second, deuteration of proteins has been demonstrated to increase DNP enhancements by a factor of 3-4.[31]

We have initiated the investigation of such an approach. In particular, in **Figure 5** we compared spectra of alanine with –CD_3 and -CH_3 methyl groups as well as between protonated and fully deuterated N-acetyl-L-Val-L-Leu. The methyl group –CH_3 of alanine disappears completely at 165 K while alanine –CD_3 signal experiences some level of attenuation but nevertheless survives. In N-Ac-VL, the Val $C_{\gamma 1}$ and $C_{\gamma 2}$ possess different activation energies, resulting in their disappearance at different temperatures, 90 K and 116 K respectively. This behavior is delayed in the perdeuterated N-Ac-VL spectra, and more importantly, valine $C_{\gamma 1}$ and $C_{\gamma 2}$ signals can still be observed at 90 K. These two carbons in N-Ac-Val were reported to have distinct E_a's of 15.3 and 22.2 kJ/mol.[38] Our results suggest that it is possible to maintain the signals from methyl

groups at low temperature by deuteration. Further investigations including the incorporation of deuterium decoupling are underway and will be the topic of the subsequent studies.

It is worth noting that the signal loss at ~243 K can be as large as ~70% in the case of bR and occurs in the neighborhood of, but above, the temperature normally associated with the protein glass transition. It appears that two mechanisms could be responsible for this effect. First, this intensity loss could be due to the freezing of glycerol/water mixture. Thus, the signal attenuation is related to the hydration of the sample and protein-water interactions and is, therefore, ubiquitous in biological samples. Second, the loss could also be due to the 2-site flipping of phenyl rings. bR contains 13 Phe's and 11 Tyr's in the amino acid sequence and preliminary ^{2}H NMR data show intermediate exchange flipping rates at this temperature. We believe this is important since protein samples are frequently studied at temperatures slightly lower than room temperature to slow some dynamic processes. Our results suggest that this approach may be suboptimal in term of the overall sensitivity. It is therefore desirable to perform such experiments at even lower temperatures, but to date, these temperatures are not always achievable due to instrumental limitations.

Finally, the main focus of this article is to address the effect of temperature on the line intensity of the –CH_3 group, along with solutions to alleviate the line-broadening effect at certain temperatures due to interference between hopping mechanism with MAS frequency and/or ^{1}H decoupling and/or CP. While such interference is problematic for some experiments, this temperature-dependent phenomena can be exploited and used to extract useful dynamic information about the system. Thus, we present here a new method to extract the activation energy of the–CH_3 group (**Figure 7**) by monitoring the change of ^{13}C signal intensities as a function of temperature. We are currently applying this novel approach to investigate the site-specific motions of other biological macromolecules like proteins, which could reveal important relations between the dynamics and functions of proteins.

CONCLUSION

In summary, we report effects of molecular motions on NMR signals of peptide and protein samples at cryogenic temperatures. In the microcrystalline tripeptide APG, a first-order polymorphic phase transition occurs at 225 K, which manifests itself in the line doubling in ^{13}C NMR spectra. At lower temperatures, we observe a destructive interference effect from the threefold jump diffusion of the Ala-CH_3 (at ~112 K) and of the Ala-NH_3^+ (at ~173 K) on the proton decoupling and/or the CP spin-lock fields. The effect on the decoupling appears to be localized, whereas the effect on the CP is readily transmitted throughout the molecule due to fast ^{1}H-^{1}H spin diffusion in a strongly coupled ^{1}H bath.

We extend these experiments to larger biological systems consisting of the membrane protein bacteriorhodopsin and amyloid fibrils formed from PI3-SH3. At ~243 K, both samples exhibit significant signal loss, in the neighborhood of the protein glass transition. Similar to the case of APG, the methyl groups are attenuated at low temperatures. However, the effect does not propagate in an obvious way to other parts of the spectrum, which supports the approach of using low temperature DNP to obtain long-range distances involving aromatic side chains. Furthermore, the intensity minima occur at lower temperatures in these biological systems than in APG (95 K vs. 112 K). Simulations of the intensity losses for the –CH_3 group in APG suggest that it should be possible to use similar data to extract site-specific information on molecular dynamics. Finally, our study suggests deuteration of the methyl groups as –CD_3 as another probe of long-range distance constraints using DNP at liquid nitrogen temperatures.

ASSOCIATED CONTENT

Supporting Information

Spin-lattice relaxation, T_1 for ^{13}C and ^{1}H measured with saturation recovery. Temperature dependence of ^{13}C Bloch decay spectra of APG. Full set of temperature-dependent ^{1}H-^{13}C CP spectra of [^{13}C,^{15}N-FVYL]-PI3-SH3. Full set of temperature-dependent ^{1}H-^{13}C CP spectra of bR.

1D ^{1}H-^{13}C CP spectra and 2D RFDR DNP spectrum of [^{13}C,^{15}N-FVYL]-PI3-SH3 fibril.

AUTHOR INFORMATION

Corresponding Author

* Robert G. Griffin, NW14-3220, 77 Massachusetts Avenue, Cambridge, MA 02139 rgg@mit.edu

Present Addresses

[3] Institute of Physical and Theoretical Chemistry, Institute of Biophysical Chemistry, and Center for Biomolecular Magnetic Resonance (BMRZ), Goethe University, 60438 Frankfurt am Main, Germany

[4]Department of Chemistry, Washington University, St. Louis, MO 63130

[5]Covaris, Woburn, MA 01801

[6]Merck Research Laboratories, West Point, PA 19486

Author Contributions

The manuscript was written through contributions of all authors. / All authors have given approval to the final version of the manuscript.

ABBREVIATIONS

MAS: magic angle spinning; NMR: nuclear magnetic resonance; ssNMR: solid state NMR; CP: cross polarization; DNP: dynamic nuclear polarization; RF: radio frequency; RFDR: radio frequency-driven recoupling; S/N: signal to noise ratio; APG: alanyl-prolyl-glycine; bR: bacteriorhodopsin; PI3-SH3: phosphatydinal-inositol-3-kinase SH3 domain

ACKNOWLEDGMENT

Funding Sources

This work was supported by grants (EB-001960, EB-002804, EB-002026 and EB-001035) from the National Institute of Biomedical Imaging and Bioengineering. B. Corzilius was partially funded by a DFG Research Fellowship CO802/1-1. K.O. Tan is supported by Early Postdoc Mobility grant -165285 provided by the Swiss National Science Foundation (SNSF).

We would like to thank Jeffrey Bryant, Ajay Thakkar and Michael Mullins for their technical assistance and Drs. Sudheer Jawla and Richard Temkin for helping with DNP instrumentation. We would like to thank Prof. Matthias Ernst for useful discussions regarding the simulations. We are grateful to Dr. Marina Belenky and Angela Jacavone for the preparation of bR, PI3-SH3 samples, respectively.

References

(1) Renault, M.; Cukkemane, A.; Baldus, M., "Solid-State Nmr Spectroscopy on Complex Biomolecules", Angew. Chem.-Int. Edit. 2010, 49, 8346-8357.

(2) Lesage, A., "Recent Advances in Solid-State Nmr Spectroscopy of Spin I=1/2 Nuclei", Phys. Chem. Chem. Phys. 2009, 11, 6876-6891.

(3) Lange, A.; Becker, S.; Seidel, K.; Giller, K.; Pongs, O.; Baldus, M., "A Concept for Rapid Protein-Structure Determination by Solid-State Nmr Spectroscopy.", Angew. Chem.-Int. Edit. 2005, 44, 2089-2092.

(4) Cady, S. D.; Schmidt-Rohr, K.; Wang, J.; Soto, C. S.; DeGrado, W. F.; Hong, M., "Structure of the Amantadine Binding Site of Influenza M2 Proton Channels in Lipid Bilayers", Nature 2010, 463, 689-U127.

(5) Castellani, F.; van Rossum, B. J.; Diehl, A.; Rehbein, K.; Oschkinat, H., "Determination of Solid-State Nmr Structures of Proteins by Means of Three-Dimensional 15n-13c-13c Dipolar Correlation Spectroscopy and Chemical Shift Analysis", Biochemistry 2003, 42, 11476-11483.

(6) Brown, S. P.; Spiess, H. W., "Advanced Solid-State Nmr Methods for the Elucidation of Structure and Dynamics of Molecular, Macromolecular, and Supramolecular Systems", Chem. Rev. 2001, 101, 4125-4155.

(7) Wel, P.; Lewandowski, J.; Griffin, R., "Solid-State Nmr Study of Amyloid Nanocrystals and Fibrils Formed by the Peptide Gnnqqny from Yeast Prion Protein Sup35p.", J. Am. Chem. Soc. 2007, 129, 5117-5130.

(8) Andreas, L. B.; Reese, M.; Eddy, M. T.; Gelev, V.; Ni, Q. Z.; Miller, E. A.; Emsley, L.; Pintacuda, G.; Chou, J. J.; Griffin, R. G., "Structure and Mechanism of the Influenza a M2(18-60) Dimer of Dimers", Journal of the American Chemical Society 2015, 137, 14877-14886.

(9) Can, T. V.; Sharma, M.; Hung, I.; Gor'kov, P. L.; Brey, W. W.; Cross, T. A., "Magic Angle Spinning and Oriented Sample Solid-State Nmr Structural Restraints Combine for Influenza a M2 Protein Functional Insights", Journal of the American Chemical Society 2012, 134, 9022-9025.

(10) De Paepe, G., "Dipolar Recoupling in Magic Angle Spinning Solid-State Nuclear Magnetic Resonance", Annu. Rev. Phys. Chem. 2012, 63, 661-684.

(11) Rienstra, C. M., "Magic-Angle Spinning Recoupling Techniques for Distance Determinations among Spin-1/2 Nuclei in Solid Peptides and Proteins", NMR Spectrosc. Biol. Solids 2006, 1-38.

(12) Ernst, M.; Meier, B. H., Adiabatic Polarization-Transfer Methods in Mas Spectroscopy. In Encyclopedia of Magnetic Resonance, John Wiley & Sons, Ltd: 2007.

(13) Bjerring, M.; Rasmussen, J. T.; Krogshave, R. S.; Nielsen, N. C., "Heteronuclear Coherence Transfer in Solid-State Nuclear Magnetic Resonance Using a Gamma-Encoded Transferred Echo Experiment", J. Chem. Phys. 2003, 119, 8916.

(14) Ernst, M., "Heteronuclear Spin Decoupling in Solid-State Nmr under Magic-Angle Sample Spinning", J. Magn. Reson. 2003, 162, 1-34.

(15) Mithu, V. S.; Pratihar, S.; Paul, S.; Madhu, P. K., "Efficiency of Heteronuclear Dipolar Decoupling Schemes in Solid-State Nmr: Investigation of Effective Transverse Relaxation Times", J. Magn. Reson. 2012, 220, 8-17.

(16) Mithu, V. S.; Paul, S.; Kurur, N. D.; Madhu, P. K., "Heteronuclear Dipolar Decoupling in Solid-State Nuclear Magnetic Resonance under Ultra-High Magic-Angle Spinning", J. Magn. Reson. 2011, 209, 359-363.

(17) Van Beek, J. D.; Carravetta, M.; Antonioli, G. C.; Levitt, M. H., "Spherical Tensor Analysis of Nuclear Magnetic Resonance Signals", J. Chem. Phys. 2005, 122, 244510/244511.

(18) Zhao, X.; Hoffbauer, W.; Schmedt auf der Gunne, J.; Levitt, M. H., "Heteronuclear Polarization Transfer by Symmetry-Based Recoupling Sequences in Solid-State Nmr", Solid State Nucl. Magn. Reson. 2004, 26, 57.

(19) Drobny, G. P.; Long, J. R.; Karlsson, T.; Shaw, W.; Popham, J.; Oyler, N.; Bower, P.; Stringer, J.; Gregory, D.; Mehta, M.; Stayton, P. S., "Structural Studies of Biomaterials Using Double-Quantum Solid-State Nmr Spectroscopy", Annu. Rev. Phys. Chem. 2003, 54, 531-571.

(20) LeMaster, D. M.; Kushlan, D. M., "Dynamical Mapping of E. Coli Thioredoxin Via 13c Nmr Relaxation Analysis", J. Am. Chem. Soc. 1996, 118, 9255-9264.

(21) Hong, M., "Determination of Multiple Φ-Torsion Angles in Proteins by Selective and Extensive 13c Labeling and Two-Dimensional Solid-State Nmr", J. Magn. Reson. 1999, 139, 389-401.

(22) Castellani, F.; van Rossum, B.; Diehl, A.; Schubert, M.; Rehbein, K.; Oschkinat, H., "Structure of a Protein Determined by Solid-State Magic-Angle-Spinning Nmr Spectroscopy.", Nature 2002, 420, 98-102.

(23) Jones, D. H.; Cellitti, S. E.; Hao, X.; Zhang, Q.; Jahnz, M.; Summerer, D.; Schultz, P. G.; Uno, T.; Geierstanger, B. H., "Site-Specific Labeling of Proteins with Nmr-Active Unnatural Amino Acids", J. Biomol. NMR 2010, 46, 89-100.

(24) Davis, L.; Chin, J. W., "Designer Proteins: Applications of Genetic Code Expansion in Cell Biology", Nat. Rev. Mol. Cell Biol. 2012, 13, 168-182.

(25) Concistre, M.; Johannessen, O. G.; Carignani, E.; Geppi, M.; Levitt, M. H., "Magic-Angle Spinning Nmr of Cold Samples", Acc. Chem. Res. 2013, 46, 1914-1922.

(26) Abragam, A., The Principles of Nuclear Magnetism. Clarendon Press: Oxford, 1961; Vol. International series of monographs on physics, p 599 p.
(27) Can, T. V.; Ni, Q. Z.; Griffin, R. G., "Mechanisms of Dynamic Nuclear Polarization in Insulating Solids", J. Magn. Reson. 2015, 253, 23-35.

(28) Gelis, I.; Vitzthum, V.; Dhimole, N.; Caporini, M. A.; Schedlbauer, A.; Carnevale, D.; Connell, S. R.; Fucini, P.; Bodenhausen, G., "Solid-State Nmr Enhanced by Dynamic Nuclear Polarization as a Novel Tool for Ribosome Structural Biology", J. Biomol. NMR 2013, 56, 85-93.

(29) Barnes, A. B.; De Paëpe, G.; van der Wel, P. C. A.; Hu, K. N.; Joo, C. G.; Bajaj, V. S.; Mak-Jurkauskas, M. L.; Sirigiri, J. R.; Herzfeld, J.; Temkin, R. J.; Griffin, R. G., "High-Field Dynamic Nuclear Polarization for Solid and Solution Biological Nmr", Applied Magnetic Resonance 2008, 34, 237-263.

(30) Maly, T.; Debelouchina, G. T.; Bajaj, V. S.; Hu, K.-N.; Joo, C.-G.; Mak-Jurkauskas, M. L.; Sirigiri, J. R.; van der Wel, P. C. A.; Herzfeld, J.; Temkin, R. J.; Griffin, R. G., "Dynamic Nuclear Polarization at High Magnetic Fields", The Journal of Chemical Physics 2008, 128, 052211-052219.

(31) Akbey, Ü.; Franks, W. T.; Linden, A.; Lange, S.; Griffin, R. G.; Rossum, B.-J. v.; Oschkinat, H., "Dynamic Nuclear Polarization of Deuterated Proteins", Angew. Chem.-Int. Edit. 2010, 49, 7803-7806.

(32) Bajaj, V. S.; Mak-Jurkauskas, M. L.; Belenky, M.; Herzfeld, J.; Griffin, R. G., "Functional and Shunt States of Bacteriorhodopsin Resolved by 250 Ghz Dynamic Nuclear Polarization-Enhanced Solid-State Nmr", Proc. Natl. Acad. Sci. U.S.A. 2009, 106, 9244-9249.

(33) Mak-Jurkauskas, M. L.; Bajaj, V. S.; Hornstein, M. K.; Belenky, M.; Griffin, R. G.; Herzfeld, J., "Energy Transformations Early in the Bacteriorhodopsin Photocycle Revealed by Dnp-Enhanced Solid-State Nmr", Proc. Natl. Acad. Sci. U.S.A. 2008, 105, 883-888.

(34) Becker-Baldus, J.; Bamann, C.; Saxena, K.; Gustmann, H.; Brown, L. J.; Brown, R. C. D.; Reiter, C.; Bamberg, E.; Wachtveitl, J.; Schwalbe, H.; Glaubitz, C., "Enlightening the Photoactive Site of Channelrhodopsin-2 by Dnp-Enhanced Solid-State Nmr Spectroscopy", Proc. Natl. Acad. Sci. U. S. A. 2015, 112, 9896-9901.

(35) Fricke, P.; Demers, J. P.; Becker, S.; Lange, A., "Studies on the Mxih Protein in T3ss Needles Using Dnp-Enhanced Ssnmr Spectroscopy", ChemPhysChem 2014, 15, 57-60.

(36) Maus, D. C.; Copie, V.; Sun, B.; Griffiths, J. M.; Griffin, R. G.; Luo, S.; Schrock, R. R.; Liu, A. H.; Seidel, S. W.; Davis, W. M.; Grohmann, A., "A Solid-State Nmr Study of Tungsten Methyl Group Dynamics in $[W(H^5\text{-}C_5me_5)Me_4][Pf_6]$", J. Am. Chem. Soc. 1996, 118, 5665-5671.

(37) Long, J. R.; Sun, B. Q.; Bowen, A.; Griffin, R. G., "Molecular Dynamics and Magic Angle Spinning Nmr", J. Am. Chem. Soc. 1994, 116, 11950-11956.

(38) Beshah, K.; Griffin, R. G., "Deuterium Quadrupole Echo Nmr Study of Methyl Group Dynamics in N-Acetyl-Dl-(Γ-D6)-Valine", J. Magn. Reson. 1989, 84, 268-274.

(39) Beshah, K.; Olejniczak, E. T.; Griffin, R. G., "Deuterium Nmr Study of Methyl Group Dynamics in L-Alanine", J. Chem. Phys. 1987, 86, 4730-4736.

(40) Linser, R.; Sarkar, R.; Krushelnitzky, A.; Mainz, A.; Reif, B., "Dynamics in the Solid-State: Perspectives for the Investigation of Amyloid Aggregates, Membrane Proteins and Soluble Protein Complexes", J. Biomol. NMR 2014, 59, 1-14.

(41) Vugmeyster, L.; Ostrovsky, D.; Ford, J. J.; Burton, S. D.; Lipton, A. S.; Hoatson, G. L.; Vold, R. L., "Probing the Dynamics of a Protein Hydrophobic Core by Deuteron Solid-State Nuclear Magnetic Resonance Spectroscopy", Journal of the American Chemical Society 2009, 131, 13651-13658.

(42) Vugmeyster, L.; Ostrovsky, D.; Khadjinova, A.; Ellden, J.; Hoatson, G. L.; Vold, R. L., "Slow Motions in the Hydrophobic Core of Chicken Villin Headpiece Subdomain and Their Contributions to Configurational Entropy and Heat Capacity from Solid-State Deuteron Nmr Measurements", Biochemistry 2011, 50, 10637-10646.

(43) Vugmeyster, L.; Ostrovsky, D.; Penland, K.; Hoatson, G. L.; Vold, R. L., "Glassy Dynamics of Protein Methyl Groups Revealed by Deuteron Nmr", J. Phys. Chem. B 2013, 117, 1051-1061.

(44) Xue, Y.; Pavlova, M. S.; Ryabov, Y. E.; Reif, B.; Skrynnikov, N. R., "Methyl Rotation Barriers in Proteins from 2h Relaxation Data. Implications for Protein Structure", J. Am. Chem. Soc. 2007, 129, 6827-6838.

(45) Latanowicz, L., "Nmr Relaxation Study of Methyl Groups in Solids from Low to High Temperatures", Concepts Magn. Reson., Part A 2005, 27A, 38-53.

(46) Andrew, E. R.; Hinshaw, W. S.; Hutchins, M. G., "Proton Magnetic-Relaxation in Crystalline Amino Acids ", J. Magn. Reson. 1974, 15, 196-200.

(47) Andrew, E. R.; Hinshaw, W. S.; Hutchins, M. G.; Sjoblom, R. O. I.; Canepa, P. C., "Proton Magnetic-Relaxation and Molecular-Motion in Polycrystalline Amino Acids 2. Alanine, Isoleucine, Leucine, Methionine, Norleucine, Threonine and Valine ", Mol. Phys. 1976, 32, 795-806.

(48) Daube, D.; Aladin, V.; Heiliger, J.; Wittmann, J. J.; Barthelmes, D.; Bengs, C.; Schwalbe, H.; Corzilius, B., "Heteronuclear Cross-Relaxation under Solid-State Dynamic Nuclear Polarization", J. Am. Chem. Soc. 2016, 138, 16572–16575.

(49) Colvin, M. T.; Silvers, R.; Ni, Q. Z.; Can, T. V.; Sergeyev, I.; Rosay, M.; Donovan, K. J.; Michael, B.; Wall, J.; Linse, S.; Griffin, R. G., "Atomic Resolution Structure of Monomorphic Aβ42 Amyloid Fibrils", Journal of the American Chemical Society 2016, 138, 9663-9674.

(50) Lehnert, E.; Mao, J. F.; Mehdipour, A. R.; Hummers, G.; Abele, R.; Glaubitz, C.; Tampe, R., "Antigenic Peptide Recognition on the Human Abc Transporter Tap Resolved by Dnp-Enhanced Solid-State Nmr Spectroscopy", Journal of the American Chemical Society 2016, 138, 13967-13974.

(51) Kaushik, M.; Bahrenberg, T.; Can, T. V.; Caporini, M. A.; Silvers, R.; Heiliger, J.; Smith, A. A.; Schwalbe, H.; Griffin, R. G.; Corzilius, B., "Gd(Iii) and Mn(Ii) Complexes for Dynamic Nuclear Polarization: Small Molecular Chelate Polarizing Agents and Applications with Site-Directed Spin Labeling of Proteins", Phys. Chem. Chem. Phys. 2016, 18, 27205-27218.

(52) Fricke, P.; Mance, D.; Chevelkov, V.; Giller, K.; Becker, S.; Baldus, M.; Lange, A., "High Resolution Observed in 800 Mhz Dnp Spectra of Extremely Rigid Type Iii Secretion Needles", J. Biomol. NMR 2016, 65, 121-126.

(53) Gochnaue, M. B.; Kushner, D. J., "Growth and Nutrition of Extremely Halophilic Bacteria", Can. J. Microbiol. 1969, 15, 1157-&.

(54) Batey, R. T.; Inada, M.; Kujawinski, E.; Puglisi, J. D.; Williamson, J. R., "Preparation of Isotopically Labeled Ribonucleotides for Multidimensional Nmr-Spectroscopy of Rna", Nucleic Acids Research 1992, 20, 4515-4523.

(55) Oesterhelt, D.; Stoeckenius, W., "Isolation of the Cell Membrane of Halobacterium Halobium and Its Fractionation into Red and Purple Membrane", Methods in enzymology 1974, 31, 667-678.

(56) Sauvee, C.; Rosay, M.; Casano, G.; Aussenac, F.; Weber, R. T.; Ouari, O.; Tordo, P., "Highly Efficient, Water-Soluble Polarizing Agents for Dynamic Nuclear Polarization at High Frequency", Angew. Chem.-Int. Edit. 2013, 52, 10858-10861.

(57) Song, C.; Hu, K.-N.; Joo, C.-G.; Swager, T. M.; Griffin, R. G., "Totapol: A Biradical Polarizing Agent for Dynamic Nuclear Polarization Experiments in Aqueous Media", Journal of the American Chemical Society 2006, 128, 11385-11390.

(58) Guijarro, J. I.; Sunde, M.; Jones, J. A.; Campbell, I. D.; Dobson, C. M., "Amyloid Fibril Formation by an Sh3 Domain", Proc. Natl. Acad. Sci. U.S.A. 1998, 95, 4224-4228.

(59) Barnes, A. B.; Mak-Jurkauskas, M. L.; Matsuki, Y.; Bajaj, V. S.; Wel, P. C. A. v. d.; DeRocher, R.; Bryant, J.; Sirigiri, J. R.; Temkin, R. J.; Lugtenburg, J.; Herzfeld, J.; Griffin, R. G., "Cryogenic Sample Exchange Nmr Probe for Magic Angle Spinning Dynamic Nuclear Polarization", J. Magn. Reson. 2009, 198, 261–270.

(60) Jawla, S.; Ni, Q. Z.; Barnes, A.; Guss, W.; Daviso, E.; Herzfeld, J.; Griffin, R.; Temkin, R., "Continuously Tunable 250 Ghz Gyrotron with a Double Disk Window for Dnp-Nmr Spectroscopy", J. Infrared Millim. Terahertz Waves 2013, 34, 42-52.

(61) Barnes, A. B.; Nanni, E. A.; Herzfeld, J.; Griffin, R. G.; Temkin, R. J., "A 250 Ghz Gyrotron with a 3 Ghz Tuning Bandwidth for Dynamic Nuclear Polarization", J. Magn. Reson. 2012, 221, 147-153.

(62) Smith, S. A.; Levante, T. O.; Meier, B. H.; Ernst, R. R., "Computer-Simulations in Magnetic-Resonance - an Object-Oriented Programming Approach", J. Magn. Reson. Ser. A 1994, 106, 75-105.

(63) Cheng, V. B.; Suzukawa, H. H.; Wolfsberg, M., "Investigations of a Nonrandom Numerical Method for Multimensional Integration ", J. Chem. Phys. 1973, 59, 3992-3999.

(64) Eddy, M.; Belenky, M.; Sivertsen, A.; Griffin, R.; Herzfeld, J., "Selectively Dispersed Isotope Labeling for Protein Structure Determination by Magic Angle Spinning Nmr", J. Biomol. NMR 2013, 57, 129-139.

(65) Lee, A. L.; Wand, A. J., "Microscopic Origins of Entropy, Heat Capacity and the Glass Transition in Proteins", Nature 2001, 411, 501-504.

(66) Markin, A. V.; Markhasin, E.; Sologubov, S. S.; Ni, Q. Z.; Smirnova, N. N.; Griffin, R. G., "Low-Temperature Polymorphic Phase Transition in a Crystalline Tripeptide L-Ala-L-Pro-Gly·H2o Revealed by Adiabatic Calorimetry", J. Phys. Chem. B 2015, 119, 1787-1792.

(67) Bajaj, V. S.; van der Wel, P. C. A.; Griffin, R. G., "Observation of a Low-Temperature, Dynamically Driven Structural Transition in a Polypeptide by Solid-State Nmr Spectroscopy", Journal of the American Chemical Society 2009, 131, 118-128.

(68) Rice, D. M.; Wittebort, R. J.; Griffin, R. G.; Meirovitch, E.; Stimson, E. R.; Meinwald, Y. C.; Freed, J. H.; Scheraga, H. A., "Rotational Jumps of the Tyrosine Sidechain in Crystalline Enkephalin H2 Nmr Lineshapes for Aromatic Rong Motion in Solids ", Journal of the American Chemical Society 1981, 103, 7707-7710.

(69) Rice, D. M.; Meinwald, Y. C.; Scheraga, H. A.; Griffin, R. G., "Tyrosyl Motion in Peptides H2 Nmr Lineshapes and Spin Lattice Relaxation ", Journal of the American Chemical Society 1987, 109, 1636-1640.

(70) Kamihira, M.; Naito, A.; Tuzi, S.; Saito, H., "Phenyl Ring Dynamics of Enkephalin Molecules and Behavior of Bound Solvents in the Crystalline States by H-2 Nmr Spectroscopy", J. Phys. Chem. A 1999, 103, 3356-3363.

(71) Bayro, M. J.; Debelouchina, G. T.; Eddy, M. T.; Birkett, N. R.; MacPhee, C. E.; Rosay, M.; Maas, W. E.; Dobson, C. M.; Griffin, R. G., "Intermolecular Structure Determination of Amyloid Fibrils with Magic-Angle Spinning and Dynamic Nuclear Polarization Nmr", Journal of the American Chemical Society 2011, 133, 13967-13974.

TOC Graphic

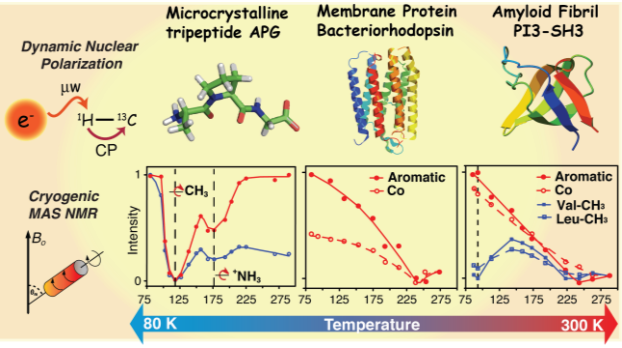
Microcrystalline tripeptide APG
Membrane Protein Bacteriorhodopsin
Amyloid Fibril PI3-SH3
Dynamic Nuclear Polarization
μW
CP
Cryogenic MAS NMR
Intensity
CH3
NH3
Aromatic
Co
Val-CH3
Leu-CH3
80 K
Temperature
300 K